

See discussions, stats, and author profiles for this publication at: <https://www.researchgate.net/publication/258850410>

# Direct Photolithography of Perfluoropolyethers for Solvent-Resistant Microfluidics

ARTICLE *in* LANGMUIR · NOVEMBER 2013

Impact Factor: 4.46 · DOI: 10.1021/la402755q · Source: PubMed

CITATIONS

7

READS

48

6 AUTHORS, INCLUDING:



**Alessandra Vitale**

Imperial College London

22 PUBLICATIONS 68 CITATIONS

SEE PROFILE



**Marzia Quaglio**

Istituto Italiano di Tecnologia

55 PUBLICATIONS 507 CITATIONS

SEE PROFILE



**Simone Luigi Marasso**

Politecnico di Torino

25 PUBLICATIONS 240 CITATIONS

SEE PROFILE



**Angelica Chiodoni**

Istituto Italiano di Tecnologia

124 PUBLICATIONS 841 CITATIONS

SEE PROFILE

# Direct Photolithography of Perfluoropolyethers for Solvent-Resistant Microfluidics

Alessandra Vitale,<sup>\*,†,‡</sup> Marzia Quaglio,<sup>\*,§</sup> Simone L. Marasso,<sup>†</sup> Angelica Chiodoni,<sup>§</sup> Matteo Cocuzza,<sup>†,§,||</sup> and Roberta Bongiovanni<sup>†,‡</sup>

<sup>†</sup>Department of Applied Science and Technology, Politecnico di Torino, C. so Duca degli Abruzzi 24, 10129 Torino, Italy

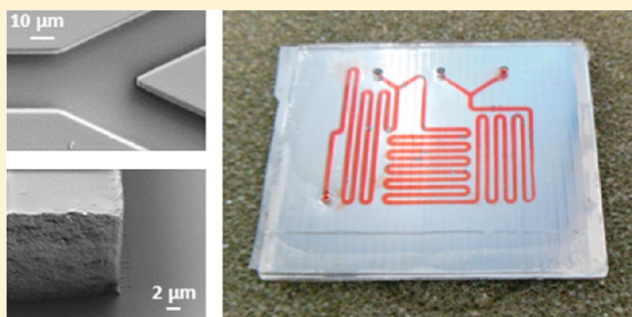
<sup>‡</sup>Consorzio Interuniversitario Nazionale per la Scienza e Tecnologia dei Materiali, Via Giusti 9, 50121 Firenze, Italy

<sup>§</sup>Center for Space Human Robotics@PoliTo, Istituto Italiano di Tecnologia, C. so Trento 21, 10129 Torino, Italy

<sup>||</sup>CNR-IMEM, Parco Area delle Scienze 37a, 43124 Parma, Italy

## Supporting Information

**ABSTRACT:** In this work, photocurable perfluoropolyethers (PFPEs) have been used for the fabrication of microfluidic devices by a direct photolithographic process. During this mask-assisted photopolymerization technique, the material is directly photopolymerized in the presence of a mask, avoiding the use of a master. We demonstrate the high level of control in transferring micropattern features with high density, a minimum transferred size of 15  $\mu\text{m}$ , a high aspect ratio (at least up to 6.5), and complex shapes useful for microfluidic applications. Moreover, we successfully apply this technology to fabricate sealed devices; the fabrication time scale for the overall process is around 5 min. The devices are able to withstand a flow pressure of up to 3.8 bar, as required for most microfluidics. Finally, the devices are tested with a model reaction employing organic solvents.



## INTRODUCTION

During the last few years, microfluidic systems have been identified as ideal investigation platforms to precisely perform, control, and analyze reactions down to the nanometer scale.<sup>1–3</sup> Polymers have assumed a leading role as the reference materials for the development and fabrication of microfluidic devices. Among them, poly(dimethylsiloxane) (PDMS) has been the most frequently used material for a wide range of applications requiring optical transparency, durability, low cost, biocompatibility, nontoxicity, and stability over a wide temperature range.<sup>4–8</sup> However, the extensive use of PDMS in the fields of chemistry and life science is limited by its very low chemical resistance.<sup>9,10</sup> Reactions performed in these reactors are limited to aqueous systems,<sup>11</sup> and a tremendous benefit could originate from the development of polymeric devices that offer the same advantages as PDMS microfluidics with the additional feature of high solvent resistance. Microreactors find increasing application in organic synthesis and drug discovery because reactions performed within microfluidic devices invariably generate relatively pure products in high yield. Solvent-resistant polymeric systems are desirable for carrying out organic-phase reactions such as polymer syntheses,<sup>12,13</sup> combinatorial chemistry reactions,<sup>14</sup> and oligonucleotide syntheses.<sup>15</sup> In 2004, Rolland and co-workers<sup>16</sup> proposed the fabrication of a novel class of microfluidic devices based on the photocurable perfluoropolyethers (PFPEs) previously described by Bongio-

vanni et al.<sup>17</sup> PFPEs can be an interesting alternative because they exhibit a low surface energy, modulus, and toxicity, high durability, toughness, and gas permeability, with the added feature of being extremely chemically resistant.<sup>15,16,18–22</sup> In particular, recent work<sup>23</sup> shows that cross-linked PFPEs have very limited swelling in several solvents, including acetone, dichloromethane, and *n*-hexane for which the solvent uptake over 1 h is 4.6, 3.2, and 0.2% w/w, respectively.

Currently PFPEs are reference materials for master replication because they grant high-quality fabrication of microfluidic devices by soft lithography with features from hundreds of micrometers<sup>16</sup> down to 100 nm.<sup>24</sup> In a soft lithography process, for the mold preparation, the polymer is poured into a master, and then it is cured either by a thermal process as with PDMS or by exposure to UV light, as in the case of PFPEs.<sup>25</sup> The master is usually obtained by a process flow made up of several technological steps involving metal deposition, optical lithography, and material etching. For typical microfluidic features, from tens to hundreds of micrometers, a photopolymerization step performed in the presence of a photomask could be an interesting alternative approach able to simplify and speed up the process significantly. Direct

Received: July 19, 2013

Revised: October 8, 2013

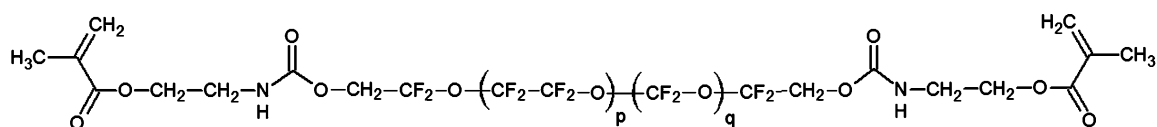


**Figure 1.** Chemical structure of PFPE methacrylate.

photolithographic methods for the fabrication of microdevices are described in the literature,<sup>26–29</sup> but these techniques are generally applied to high-modulus materials. We have already demonstrated that a similar approach is possible with low-modulus UV-curable PFPE, preserving the properties of the material.<sup>23</sup>

In this work, we used a commercial UV-curable bifunctional methacrylic PFPE for the fabrication of microfluidic structures, demonstrating that a high accuracy in pattern transfer is possible by controlling the UV-induced curing reaction via a photolithographic approach. We selected silicon wafers as substrate material, and adhesion between the fluorinated polymer and the substrate was increased by a surface functionalization step.<sup>23</sup> We developed this direct photolithographic approach in designing a mask with typical microfluidic-like structures, demonstrating its strength with respect to the existing photolithographic methods:<sup>26–29</sup> the aspect ratio was 6.5, the minimum dimension of the feature obtained was 15  $\mu\text{m}$  with a side angle of 90°, and complex shapes and high-density patterns could be fabricated. Moreover, the overall time for completing the building of the entire device was about 5 min. We successfully tested the mask-assisted photopolymerization technique fabricating a complete microfluidic device: as a proof of principle, the device was employed to run a model reaction and demonstrated its functionality for solvent-resistant microfluidics.

## EXPERIMENTAL SECTION

Bifunctional methacrylate-PFPE macromer (Fluorolink MD 700 by Solvay-Solexis) was added to 4% w/w photoinitiator 2-hydroxy-2-methyl-1-phenyl-propan-1-one (Sigma-Aldrich) to obtain the final photocurable reactive mixture. The chemical structure of PFPE is reported in Figure 1. Silicon wafers were selected as substrate materials. To increase the adhesion of photocurable PFPE, a functionalization step was performed on the wafer using methacryloxy propyl trimethoxysilane (MPTMS) as described elsewhere.<sup>23</sup>

PFPE was spin coated on functionalized silicon using a Delta BM20 spinner by B.L.E Equipment. The spinning curve of the material is reported in a previous work:<sup>23</sup> a 20- $\mu\text{m}$ -thick layer can be obtained with a spinning speed of 1000 rpm, a spinning time of 50 s, and an acceleration of 500 rpm  $\text{s}^{-1}$ .

The photolithographic process was optimized using quartz masks, with test patterns having different geometries and dimensions. As a reference for the energy dose selection, the quartz mask reported in Figure 2a was used. All of the lines in the mask are 25  $\mu\text{m}$  wide and are organized in different structures. Three patterns of straight lines can be observed, each with a different distance ( $d$ ) between two adjacent lines of 25, 50, and 75  $\mu\text{m}$ . Another pattern is proposed with lines intersecting at 90°. The designed mask also contains isolated circular structures (a circle with an outer ring) and lines crossing at different angles mimicking the structure of diffusion-based mixers: the intersections are at 30, 45, or 90°.

Exposure was performed under an inert atmosphere (nitrogen) using a high-pressure mercury arc lamp by Osram (intensity of 5 mW  $\text{cm}^{-2}$  and broadband emission showing all the three main lines g–i). The exposure system is sketched in Figure 2b: it is a manual exposure system consisting of the above-described UV lamp, a condenser lens, and a mirror to direct the light beam onto the sample. The kinetics of the photopolymerization reaction of the PFPE macromer was studied

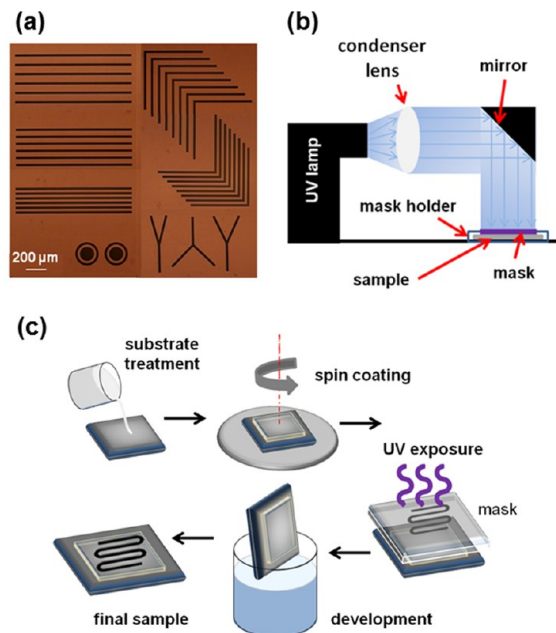


**Figure 2.** (a) Optical image of the quartz mask used to select the energy dose. (b) Sketch of the homemade exposure setup. (c) Process flow for the optimized direct photolithographic process.

by Fourier transform infrared (FTIR) analysis using a Thermo-Nicolet 5700 instrument. The conversion was calculated by monitoring the decrease in the area of the absorption band of the reactive functionality (methacrylate C=C peak at 1640  $\text{cm}^{-1}$ ) with time.

The development was carried out in acetone, chosen according to swelling experiments reported elsewhere.<sup>23</sup> Pattern analyses were performed with a Nikon Eclipse ME600 optical microscope, and an Auriga (Zeiss) field emission scanning electron microscope (FESEM). Prior to FESEM examination, samples were coated with an 8-nm-thick Au film via sputtering.

The patterned films were then sealed by placing them in contact with a 1-mm-thick slab made of the same fluoropolymer subjected to uncomplete UV curing: the system was aligned and then exposed again to UV light. The 1-mm-thick slab had inlet and outlet holes; it was obtained by pouring the PFPE monomer into a poly(methyl methacrylate) mold. To test the quality of the bonding procedure, we performed a static test in order to evaluate the maximum sustainable pressure of a simple microfluidic structure made of a straight microchannel. The setup for characterization consisted of a syringe pump (twin syringe precision pump model 33, Harvard Apparatus), a piezoresistive pressure sensor (Honeywell model 26PCFFA6G), and a multimeter (Agilent Technology 34970A) for data acquisition. Low-density polyethylene (LDPE) tubes were used to connect the device to the system. During the test, the channel was filled with colored water in order to check the leakage by eye; a manual valve was employed to switch from waste to sensor connector by ensuring the complete filling of the microchannel (details in the Supporting Information).

To evaluate the resistance of devices at high temperature, we filled them with water, sealed the inlet and outlet holes to avoid any fluid leaving, heated the systems to 90 °C for up to 30 min, and weighted the water inside the channel after cooling to room temperature to control whether leakage was occurred. Moreover, we tested the

stability of the devices simply by depositing them in a heater and examining the temperature at which device failure occurred.

To test the device, the photoinitiation of benzophenone was chosen as a model system. A device with a serpentine shape was designed to yield a long channel with a large surface area. The channel was 500  $\mu\text{m}$  wide and 96  $\mu\text{m}$  deep. Benzophenone and isopropanol purchased from Sigma-Aldrich were used without further purification. A 0.1 M benzophenone solution in isopropanol was prepared with the addition of a drop of glacial acetic acid (Sigma-Aldrich). Before each run, nitrogen was bubbled through the reactant solution for at least 10 min to deoxygenate the solution. The device was filled with reactant solution at a flow rate of 5  $\mu\text{L min}^{-1}$  and irradiated with UV light (Hamamatsu LC8, light intensity of 250  $\text{mW cm}^{-2}$ ) for different times. The samples were then collected by drawing the reaction mixture from the device. The reaction was monitored by UV analysis (using a ATI Unicam UV2 spectrophotometer) 24 h after collection to ensure the completion of dark reactions (reaction steps following initial light exposure but not involving photons).<sup>30</sup>

## RESULTS AND DISCUSSION

PFPE methacrylate is a commercial photosensitive macromer proposed for polymer modifications and surface treatments.<sup>31</sup> It cannot be considered to be a photoresist, but because it undergoes photopolymerization when exposed to UV light, its behavior can be compared to that of a negative photoresist. The interest in using PFPEs in microfluidics is justified by their peculiar properties, including a low modulus and outstanding chemical resistance.<sup>23</sup> The elastomeric behavior of cross-linked PFPE (with a Young's modulus of 9.4 MPa) could allow the direct incorporation of moving parts as valves and pumps into the devices. However, the high solvent resistance could widen microfluidics applications in the field of chemical reactions.

In a standard UV-lithography process, the actual shape and dimensions of the patterned features are controlled by fine-tuned steps. Substrate pretreatment, spin coating, soft bake, UV exposure, postexposure bake (PEB), development, and hard bake are the main steps each corresponding to well-known changes in the photoresist. In processing a PFPE methacrylate, no thermal step is necessary to stabilize the material before exposure because the prepolymer does not contain solvents. Moreover, because of the very low  $T_g$  of the cross-linked polymer ( $T_{g1} = -88\text{ }^\circ\text{C}$  and  $T_{g2} = 29\text{ }^\circ\text{C}$ ),<sup>32</sup> methacrylic PFPE does not stabilize stationary waves during UV exposure so that no PEB step is required. The hard bake treatment is substituted by an additional UV exposure step, named postlithography curing, that can complete the cross-linking of PFPE methacrylate. The resulting process flow, described in Figure 2c, is significantly simpler than that usually adopted in standard optical lithography. We assessed the mask-assisted photopolymerization process using the manual exposure system shown in Figure 2b by blowing nitrogen into the mask holder room without the need for stringent conditions, thus ensuring an easily reproducible process. The fabrication time scale for the overall process is around 5 min, which is much shorter than both standard photolithography processes with commercial photoresists and similar UV-based rapid prototyping techniques<sup>27,29</sup> that require a baking step.

We worked with a PFPE methacrylate layer of 20  $\mu\text{m}$ , obtained with a spinning speed of 1000 rpm. The selected substrate was a Si wafer pretreated with MPTMS, an alkoxysilane containing an acrylic functionality able to coreact with methacrylic PFPE.

The mask-assisted photopolymerization process can be accurately controlled only after obtaining detailed knowledge

of the behavior of the photocurable reactive mixture under UV light. The photopolymerization conversion curve of a 20- $\mu\text{m}$ -thick PFPE film is reported in Figure 3. It shows that by

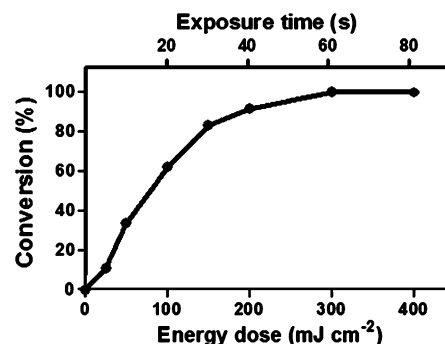


**Figure 3.** Photopolymerization conversion curve for a 20- $\mu\text{m}$ -thick methacrylic PFPE film.

increasing the energy dose, which is proportional to the exposure time, the photopolymerization reaction progresses and the conversion of the macromer to the polymer advances. Above 300  $\text{mJ cm}^{-2}$ , the conversion of the product is complete and a fully cross-linked material is obtained. As expected, the kinetics of photopolymerization depends on the film thickness (Figure S1 in the Supporting Information): the thicker the PFPE, the slower the speed of the conversion reaction. However, the photopolymerization reaction is quite fast even with thick films, and a complete conversion is reached for any thickness.

Obviously, during exposure the photopolymerization reaction is induced only where UV rays can reach the material, and the macromer and the photoinitiator do not react where the radiation is blocked by the mask. Therefore, the selection of the energy dose must be performed not only by considering the conversion degree but also by analyzing the shape of the features obtained. To optimize the exposure time, we selected the straight-line patterns in the quartz mask of Figure 2a as the reference structures. As the distance ( $d$ ) between the lines decreases, the feature density increases and the complexity of the optical pattern transfer increases as well. Each line in the mask is a UV-blocking element, so the macromer under it cannot polymerize, resulting in an opening, analogous to a microchannel, in the final sample. The FESEM analysis of the 20- $\mu\text{m}$ -thick straight-line patterns as a function of the energy dose is reported in Figure 4. Three different energy doses are taken into consideration: 105, 125, and 165  $\text{mJ cm}^{-2}$ . At 105  $\text{mJ cm}^{-2}$ , the energy dose is not sufficient for pattern transfer: the microchannels are wider than the nominal dimension, or the ridges are even nonexistent. At 165  $\text{mJ cm}^{-2}$ , the energy dose is too high: the ridges are wider than the nominal dimension or the microchannels are even filled with polymerized material. The lack of definition is likely to be due to the diffusion of the oligomer into the dark areas: although the diffusion coefficient of the system is not known, we can estimate that it is high as the  $T_g$  of both the unreacted oligomer and the cross-linked polymer, which is very low. Therefore, the optimum energy dose for transferring lines with different  $d$  values is 125  $\text{mJ cm}^{-2}$ . The actual size and shape of the transferred structures are very close to the nominal ones on the photomask, with the variation being close to 1%.

By analyzing Figure 4, it is also possible to notice the extremely high contrast of methacrylic PFPE. The contrast is a



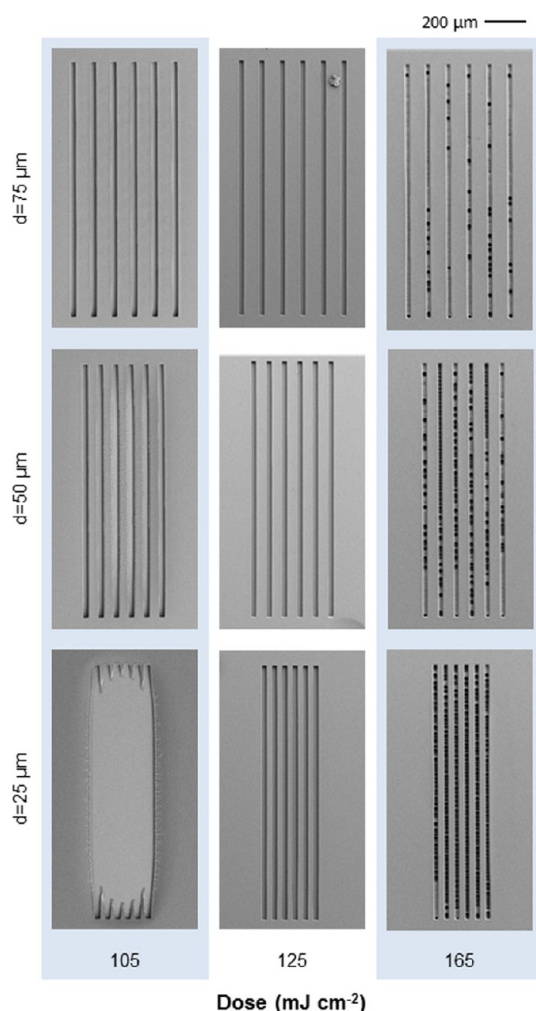


**Figure 4.** FESEM analysis of the straight-line patterns exposed to different energy doses: 105, 125, and 165  $\text{mJ cm}^{-2}$ , corresponding to 21, 25, and 33 s, respectively.

measure of the resolving power of a photoresist and describes its ability to distinguish between light and dark areas. This property is hence quite important because it is related to the capability of fabricating high-aspect-ratio structures. As a demonstration, patterns thicker than 20  $\mu\text{m}$  with a very high lateral resolution are presented (Figure S2 in the Supporting Information).

By observing Figure 4, it is evident that an energy dose of 300  $\text{mJ cm}^{-2}$  (minimum dose required to complete the photopolymerization reaction, see Figure 3) is too great to obtain good pattern transfer. Therefore, because the optimum energy dose for pattern transfer is not sufficient to obtain complete photopolymerization, the resulting polymer does not exhibit its optimal chemical, thermal, and mechanical properties. In this case, a postlithography curing step can be introduced. After the development of the patterned film, the sample can be exposed again to UV light without any mask. In this way, the material reaches its maximum conversion degree, maintaining the patterned features. The dimensional variation after postlithography curing is less than 3%. The effect of postlithography curing on straight lines is shown in Figure 5a. If the sample is not completely cross-linked (image  $a_I$ ), then some wrinkles at the edge features are present: it is likely that they form during FESEM analysis because the electronic beam can

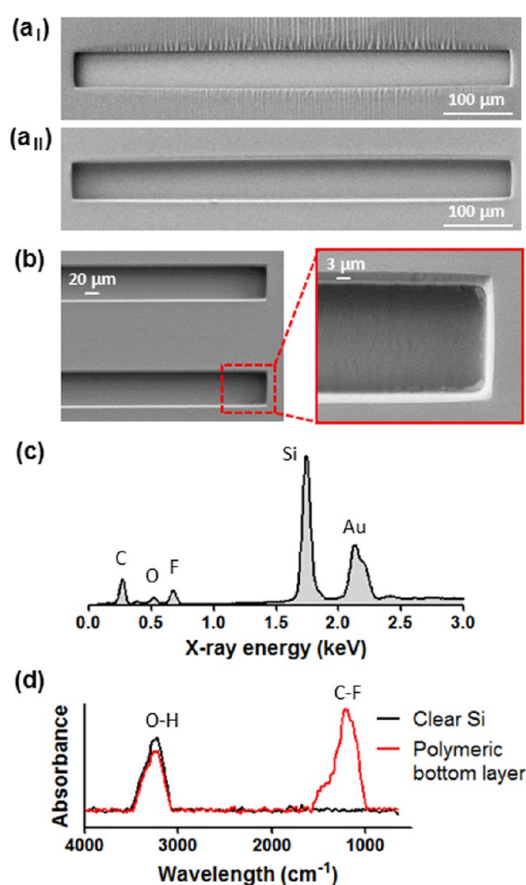


**Figure 5.** (a) Straight microchannel before ( $a_I$ ) and after ( $a_{II}$ ) the postlithography curing step is proposed. (b) The morphology of the thin film spontaneously formed at the bottom of the microchannel is analyzed by FESEM. Its fluorinated composition is verified by (c) EDX and (d) FT-IR analyses, respectively.

damage the material. Otherwise, if the sample is fully cured (i.e., subjected to postlithography curing), then such wrinkles are not formed (image  $a_{II}$ ).

During the mask-assisted photopolymerization process, a thin PFPE polymeric film is formed at the bottom of the microchannels. This thin layer can be observed by FESEM characterization as shown in Figure 5b. Its presence is also confirmed by EDX and FT-IR analysis (Figure 5c,d, respectively). Both spectra show peaks related to the presence of fluorine on the surface of the Si substrate. This thin fluorinated film makes the chemical properties of the bottom surface of the polymeric microchannel similar to that of its other sides, which is a fundamental requirement for performing real microfluidic reactions and life science protocols. Because the Si wafer used as a substrate is functionalized with an acrylic alkoxyisilane<sup>23</sup> that coreacts with the PFPE oligomer, the layer at the bottom of the channel is chemically bonded to the substrate. In fact, it cannot be washed away by water or other solvents. Also during the development there is no detachment from the surface; it is worth noticing that the pattern itself has good adhesion although it is highly fluorinated and has a low surface tension. This suggests a chemical bonding of the PFPE polymer to the modified Si wafer.

We used the optimum dose of 125  $\text{mJ cm}^{-2}$  to transfer into 20- $\mu\text{m}$ -thick layers of PFPE methacrylate the other patterns and structures of the mask in Figure 2a. All of the obtained shapes are precise, regular, and reproducible as proposed in

Figure 6a: enlargements of mixerlike structures with 30, 45, and 90° intersections, curved lines, and a 90° intersecting line

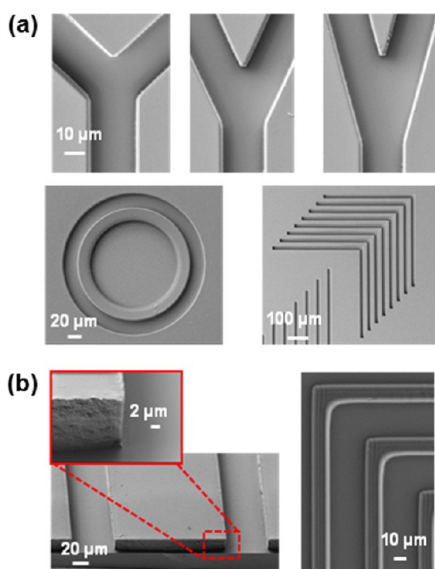


Figure 6. (a) The test of pattern transfer by mask-assisted photopolymerization process is proposed, showing enlargements of mixerlike structures with 30, 45, and 90° intersections, curved lines, and a 90° intersecting line pattern. (b) The analysis of a microchannel section and sidewall and the pattern of 15-μm-wide lines are proposed: this is the minimum transferred structure tested in this work.

pattern are shown. In Figure 6b, the section of the straight-line pattern reveals the vertical sidewalls of the microchannels. A pattern of 15-μm-wide lines was also tested in order to verify the ability of the process to transfer features smaller than 25 μm. In Figure 6b, the 15-μm-wide pattern reproduced into a 20-μm-thick PFPE layer is shown: this is the minimum size analyzed in this work.

For microfluidic applications, channels with a thickness greater than 20 μm are often required. For this reason, we developed a double-spinning process—a technique that is rarely used for commercial resists—in order to increase the final thickness of the polymeric layer. The first spin-coating process of the material is performed to get a 20-μm-thick layer: this is the selected first working layer (Figure 7a); then the liquid macromer is added and a second spinning process follows. Finally, the double-spun system is exposed to UV light to obtain a completely continuous and homogeneously thick PFPE layer. The thickness resulting from this double-spinning process is plotted in Figure 7b; films with a total thickness of up to 96 μm can be produced.

In our previous work,<sup>23</sup> we demonstrated that the single-spinning curve of PFPE methacrylate follows the simple Emslie model<sup>33</sup> in the case of an initially uniform distribution. We noticed that the double-spinning curve of the same material does not follow the same law. In fact, the model does not take into account the surface energy of the substrate, which is usually greater than that of the photoresist. On the contrary, in the double-spinning process the substrate is the spun liquid PFPE macromer whose surface energy is only  $23.7 \pm 0.3$  mN m<sup>-1</sup>. To the best of our knowledge, in the literature spinning models appropriate for low-surface-energy substrates are not reported.

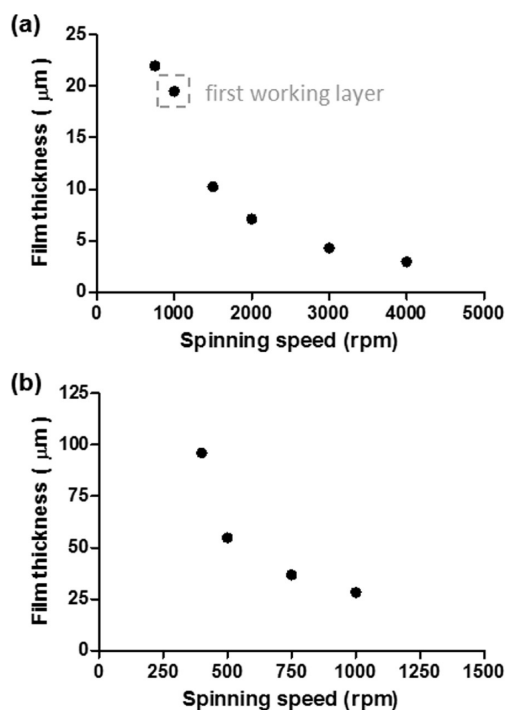


Figure 7. (a) Single-spinning curve of methacrylic PFPE. (b) Double-spinning curve of methacrylic PFPE, obtained from the selected first working layer (20-μm-thick spun film).

With a thickness of 96 μm, the mask-assisted photopolymerization process was used to UV pattern a filter structure made of microchannels with columns both in the middle and partially embedded in the sidewall. The images of this sample are reported in Figure 8: the channel is 200 μm

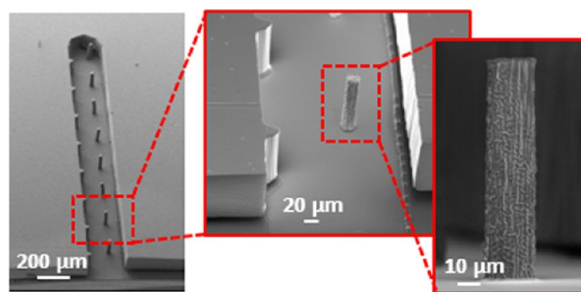
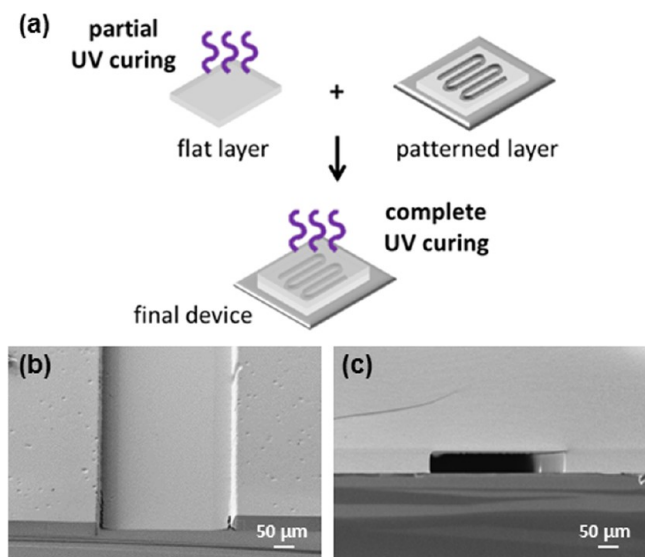


Figure 8. Test pattern for a filter structure; a 6.5 aspect ratio can be observed.

wide, and the cylinder diameter is 15 μm. The selected energy dose required to UV pattern such structure is 300 mJ cm<sup>-2</sup>. The columns are accurately reproduced and identical, not only demonstrating the ability to reproduce 15-μm-wide structures even in this thicker layer but also proving that an aspect ratio of up to 6.5 is achievable with PFPE methacrylate by this process. It is important to underline the precision of the vertical microchannel walls, both when they are plain and when they contain half-cylinders, with a sidewall angle close to 90°. Moreover, with our direct photolithographic process we have shown the achievement of smaller features compared to those presented in the literature in work involving direct photolithography for microfluidics.<sup>26</sup>

We sealed the microfluidic structures by the bonding procedure described in our previous work<sup>23</sup> using a flat (1-

mm-thick), uncured PFPE layer exposed to UV light for a very short time (60 s with a light intensity of  $27 \text{ mW cm}^{-2}$ ). The flat layer is deposited onto the patterned layer, and the system is exposed again to UV light without applying any pressure (Figure 9a). This exposure step allows us to chemically



**Figure 9.** (a) Bonding procedure. Section of a microfluidic channel (b) before and (c) after bonding.

bond the two layers together, and it includes the postlithography curing step as well. In Figure 9, we propose an example of a  $300 \mu\text{m} \times 55 \mu\text{m}$  PFPE microfluidic channel before (Figure 9b) and after (Figure 9c) bonding. The sealing in the interchannel area is clearly satisfactory: the microchannel geometry is retained, and the polymeric material results are homogeneous and continuous.

We decided to evaluate the quality of the bonding procedure by estimating the maximum sustainable pressure before leakage. We fabricated a simple microfluidic structure made of a 1-cm-long,  $200\text{-}\mu\text{m}$ -wide,  $55\text{-}\mu\text{m}$ -high straight channel produced on silicon by our photolithographic process using the double-spinning procedure and closed it with a 1-mm-thick PFPE layer with inlet and outlet holes manufactured by casting. A clamping system was designed and used to optimize the positioning of the tubes in the channel. The assembly was as easy to make as with PDMS: in fact, the PFPE polymer is soft and exhibits elastomeric behavior. The final system is shown in Figure 10a. We performed a pressure test, as described previously, with a closed end circuit connected to the straight microchannel. The pressure measurement was stopped when the maximum sustainable pressure was reached (Figure 10b). The tests were performed on different samples by maintaining a flow rate of  $30 \mu\text{L}/\text{min}$  until leakage was observed. In all of the bonding strength tests, the leakage occurred at the interface between the tubes and the microchannel inlet or outlet. Therefore, the maximum sustainable pressure was assumed to be 3.8 bar because it was the maximum measured pressure. Moreover we confirmed that the maximum pressure sustainable by the system is not dependent on the flow rate (Figure S4 in Supporting Information). The maximum pressure of 3.8 bar appears to be very favorable to a microfluidic device because in different works applied pressure both to fluorinated- and PDMS-based systems is lower,<sup>15,18,34,35</sup> while microfluidic

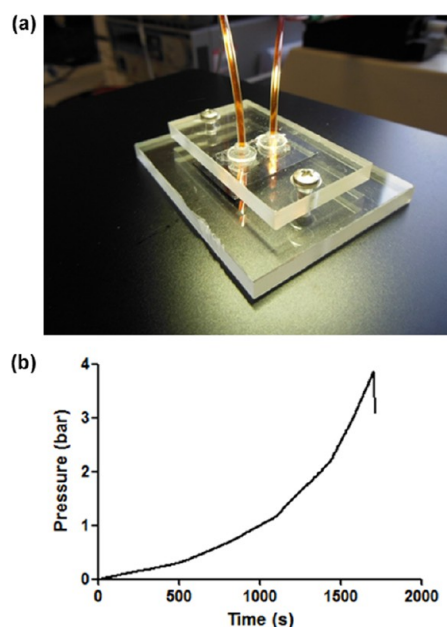


**Figure 10.** Evaluation of the maximum sustainable pressure. (a) The clamping system is reported, showing the tubes with the colored solution connected to the device. (b) The curve representing the pressure increasing in the system while blocking the outlet tube and pumping water at a constant flow rate of  $30 \mu\text{L min}^{-1}$ .

devices made of more rigid materials can sustain even higher pressures.<sup>11,36</sup>

We also evaluated the stability of the device at higher temperatures. In particular, we analyzed a device filled with water and held at  $90^\circ\text{C}$  for 10 min, a typical thermal step required for DNA amplification.<sup>8</sup> Moreover, we tested the resistance of the device at the same temperature for longer times (up to 30 min), demonstrating that it resists well without fluid leakage, swelling, or distortion. The devices can sustain a temperature of up to  $125^\circ\text{C}$  before damage and delamination from the silicon substrate.

We decided to test the mask-assisted photopolymerization process for the fabrication of a complete microfluidic device. We selected the layout of the multi-inlet lab on a chip (LOC) with a passive micromixer based on a bare, straight microchannel integrating a “Y” inlet junction: this is a structure that is already used in a DNA hybridization protocol.<sup>37</sup> The PFPE LOC is shown in Figure 11. In Figure 11a, an image of the final device is proposed to show the high quality of the pattern transferred by this photolithographic approach. The final LOC after filling with a colored solution is proposed in Figure 11b. We prepared this sealed microfluidic device through a very simple technology that requires few processing steps and uses

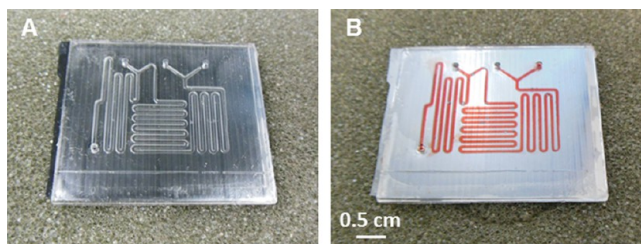


**Figure 11.** PFPE LOC (a) before and (b) after filling with colored-water-based solution.



fast UV curing both for the pattern transfer and for the bonding step.

To test the functionality of the fabricated devices, the benzopinacol formation reaction via the photoreduction of benzophenone in isopropanol was used as a model reaction (reaction scheme in Figure 12a). Hydrogen abstraction by

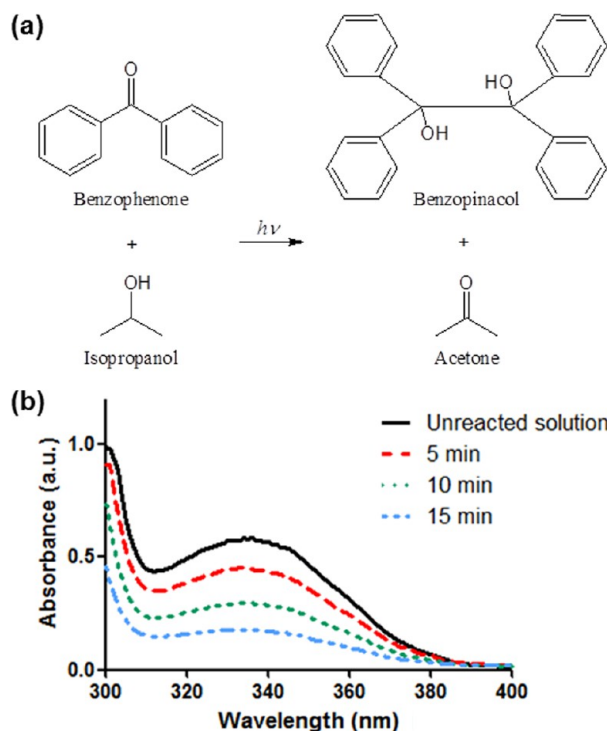


**Figure 12.** (a) Reaction scheme of the photopinacolation of benzophenone in isopropanol. (b) UV absorption of the reaction mixture at different UV irradiation times.

photoexcited benzophenone from isopropanol yields benzopinacol and acetone as stable products.<sup>30,38</sup> The improvement in the applicability and efficiency of photochemical reactions, such as the one selected, by using microfluidics has already been described.<sup>30</sup> A serpentine-like pattern with the same dimensions of the device in Figure 11 was selected for the reactor to yield a large surface area and therefore to receive the maximum amount of light possible. The reaction needs only initiation with UV light and then propagates with radicals (dark reaction). Figure 12b shows the UV absorption of the reaction mixture at different exposure times. The disappearance of the peak at 330 nm can be correlated to the conversion of benzophenone. UV spectra do not show the presence of highly absorbant intermediates because they are oxygen-sensitive and are destroyed as a result of the exposure of the systems to oxygen before analyses. The results of Figure 12b obviously demonstrate that the conversion of benzophenone is a function of the UV irradiation time. The longer the irradiation time, the greater the conversion of reactants as expected.

## CONCLUSIONS

In this work, we demonstrate that a robust and well-controlled pattern-transfer technique based on a direct photolithographic approach can be applied to PFPE methacrylate.

The dimensions and the shape of the final pattern can be tuned and optimized by controlling the energy dose (exposure

time), granting at the same time a complete polymerization of the material. We have tested this mask-assisted photopolymerization process for different microfluidic features and always obtain regular and precise patterns. Moreover, microstructures with an aspect ratio of at least up to 6.5 can be fabricated. The proposed bonding procedure is demonstrated to be efficient, guaranteeing high-pressure resistance for the sealed microfluidic devices. Finally, we used the mask-assisted photopolymerization process to fabricate complete LOCs for chemical synthesis applications, and the solvent-resistant devices were successfully tested for the benzopinacol formation reaction via the photoreduction of benzophenone in isopropanol. With this simple photochemical model reaction, we demonstrated that PFPE devices fabricated through the direct photolithography process have a promising potential for application in microfluidic organic synthesis.

## ASSOCIATED CONTENT

### Supporting Information

Additional details on the photopolymerization conversion, pattern transfer, and bonding strength tests. This material is available free of charge via the Internet at <http://pubs.acs.org>.

## AUTHOR INFORMATION

### Corresponding Authors

\*E-mail: [alessandra.vitale@polito.it](mailto:alessandra.vitale@polito.it)

\*E-mail: [marzia.quaglio@iit.it](mailto:marzia.quaglio@iit.it)

### Author Contributions

This manuscript was written through the contributions of all authors. All authors have given approval to the final version of the manuscript.

### Notes

The authors declare no competing financial interest.

## ACKNOWLEDGMENTS

We gratefully acknowledge the Consorzio INSTM for partially funding A.V.'s fellowship. We thank Solvay Specialties for providing the macromer.

## REFERENCES

- (1) Reyes, D. R.; Iossifidis, D.; Auroux, P.-A.; Manz, A. Micro total analysis systems. 1. Introduction, theory, and technology. *Anal. Chem.* **2002**, *74*, 2623–2636.
- (2) deMello, A. J. Control and detection of chemical reactions in microfluidic systems. *Nature* **2006**, *44*, 394–402.
- (3) Whitesides, G. M. The origins and the future of microfluidics. *Nature* **2006**, *442*, 368–373.
- (4) Jo, B. H.; Van Lerberghe, L. M.; Motsegood, K. M.; Beebe, D. J. Three-dimensional micro-channel fabrication in polydimethylsiloxane (PDMS) elastomer. *J. Microelectromech. Syst.* **2000**, *9*, 76–81.
- (5) deMello, A. J. Plastic fantastic? *Lab Chip* **2002**, *2*, 31N–36N.
- (6) Domachuk, P.; Tsioris, K.; Omenetto, F. G.; Kaplan, D. L. Bio-microfluidics: biomaterials and biomimetic designs. *Adv. Mater.* **2010**, *22*, 249–260.
- (7) Zhang, X.; Haswell, S. J. Materials matter in microfluidic devices. *MRS Bull.* **2006**, *31*, 95–99.
- (8) Pasquardini, L.; Potrich, C.; Quaglio, M.; Lamberti, A.; Guastella, S.; Lunelli, L.; Cocuzza, M.; Vanzetti, L.; Pirri, C. F.; Pederzoli, C. Solid phase DNA extraction on PDMS and direct amplification. *Lab Chip* **2011**, *11*, 4029–4035.
- (9) Lee, J.; Park, C.; Whitesides, G. M. Solvent compatibility of poly(dimethylsiloxane)-based microfluidic devices. *Anal. Chem.* **2003**, *75*, 6544–6554.



- (10) Kim, B.-Y.; Hong, L.-Y.; Chung, Y.-M.; Kim, D.-P.; Lee, C.-S. Solvent-resistant PDMS microfluidic devices with hybrid inorganic/organic polymer coatings. *Adv. Funct. Mater.* **2009**, *19*, 3796–3803.
- (11) Sollier, E.; Murray, C.; Maoddi, P.; Di Carlo, D. Rapid prototyping polymers for microfluidic devices and high pressure injections. *Lab Chip* **2011**, *11*, 3752–3765.
- (12) Hoang, P. H.; Nguyen, C. T.; Perumala, J.; Kim, D.-P. Droplet synthesis of well-defined block copolymers using solvent-resistant microfluidic device. *Lab Chip* **2011**, *11*, 329–335.
- (13) Wu, T.; Mei, Y.; Cabral, J. T.; Xu, C.; Beers, K. L. New synthetic method for controlled polymerization using a microfluidic system. *J. Am. Chem. Soc.* **2004**, *126*, 9880–9881.
- (14) Ueno, K.; Kitagawa, F.; Kitamura, N. Photocyanation of pyrene across an oil/water interface in a polymer microchannel chip. *Lab Chip* **2002**, *2*, 231–234.
- (15) Huang, Y.; Castrataro, P.; Lee, C.-C.; Quake, S. R. Solvent resistant microfluidic DNA synthesizer. *Lab Chip* **2007**, *7*, 24–26.
- (16) Rolland, J. P.; Van Dam, R. M.; Schorzman, D. A.; Quake, S. R.; DeSimone, J. M. Solvent-resistant photocurable “liquid Teflon” for microfluidic device fabrication. *J. Am. Chem. Soc.* **2004**, *126*, 2322–2323.
- (17) Priola, A.; Bongiovanni, R.; Malucelli, G.; Pollicino, A.; Tonelli, C.; Simeone, G. UV-curable systems containing perfluoropolyether structures: synthesis and characterisation. *Macromol. Chem. Phys.* **1997**, *198*, 1893–1907.
- (18) Maltezos, G.; Garcia, E.; Hanrahan, G.; Gomez, F. A.; Vyawhare, S.; van Dam, R. M.; Chen, Y.; Scherer, A. Design and fabrication of chemically robust three-dimensional microfluidic valves. *Lab Chip* **2007**, *7*, 1209–1211.
- (19) De Marco, C.; Girardo, S.; Mele, E.; Cingolani, R.; Pisignano, D. Ultraviolet-based bonding for perfluoropolyether low aspect-ratio microchannels and hybrid devices. *Lab Chip* **2008**, *8*, 1394–1397.
- (20) Devaraju, N. S. G. K.; Unger, M. A. Multilayer soft lithography of perfluoropolyether based elastomer for microfluidic device fabrication. *Lab Chip* **2011**, *11*, 1962–1967.
- (21) Renckens, T. J. A.; Janeliunas, D.; van Vliet, H.; van Esch, J. H.; Mul, G.; Kreutzer, M. T. Micromolding of solvent resistant microfluidic devices. *Lab Chip* **2011**, *11*, 2035–2038.
- (22) Xiao, Z.; Zhao, Y.; Wang, A.; Perumal, J.; Kim, D.-P. Practical approach for macroporous structure embedded microfluidic system and the catalytic microchemical application. *Lab Chip* **2011**, *11*, 57–62.
- (23) Vitale, A.; Quaglio, M.; Cocuzza, M.; Pirri, C. F.; Bongiovanni, R. Photopolymerization of a perfluoropolyether oligomer and photolithographic processes for the fabrication of microfluidic devices. *Eur. Polym. J.* **2012**, *48*, 1118–1126.
- (24) Rolland, J. P.; Hagberg, E. C.; Denison, G. M.; Carter, K. R.; De Simone, J. M. High-resolution soft lithography: enabling materials for nanotechnologies. *Angew. Chem., Int. Ed.* **2004**, *43*, 5796–5799.
- (25) Rolland, J. P.; Maynor, B. W.; Euliss, L. E.; Exner, A. E.; Denison, G. M.; DeSimone, J. M. Direct fabrication and harvesting of monodisperse, shape-specific nanobiomaterials. *J. Am. Chem. Soc.* **2005**, *127*, 10096–10100.
- (26) Khoury, C.; Mensing, G. A.; Beebe, D. J. Ultra rapid prototyping of microfluidic systems using liquid phase photopolymerization. *Lab Chip* **2002**, *2*, 50–55.
- (27) Harrison, C.; Cabral, J. T.; Stafford, C. M.; Karim, A.; Amis, E. J. A rapid prototyping technique for the fabrication of solvent-resistant structures. *J. Micromech. Microeng.* **2004**, *14*, 153–158.
- (28) Hutchison, J. B.; Haraldsson, K. T.; Good, B. T.; Sebra, R. P.; Luo, N.; Anseth, K. S.; Bowman, C. N. Robust polymer microfluidic device fabrication via contact liquid photolithographic polymerization (CLiPP). *Lab Chip* **2004**, *4*, 658–662.
- (29) Schmidt, L. E.; Yi, S.; Jin, Y.-H.; Leterrier, Y.; Cho, Y.-H.; Manson, Y.-A. E. Acrylated hyperbranched polymer photoresist for ultra-thick and low-stress high aspect ratio micropatterns. *J. Micromech. Microeng.* **2008**, *18*, 045022–045029.
- (30) Lu, H.; Schmidt, M. A.; Jensen, K. F. Photochemical reactions and on-line UV detection in microfabricated reactors. *Lab Chip* **2001**, *1*, 22–28.
- (31) Koo, N. V. A.; Plachetka, U. P. M.; Moormann, C. N. A. Nanolithography process. WO 2010/094661 A1, 2010.
- (32) Vitale, A.; Priola, A.; Tonelli, C.; Bongiovanni, R. Nano-heterogeneous networks by photopolymerization of perfluoropolyethers and acrylic co-monomers. *Polym. Int.* **2013**, *62*, 1395–1401.
- (33) Emslie, A. G.; Bonner, F. T.; Peck, L. G. Flow of a viscous liquid on a rotating disk. *J. Appl. Phys.* **1958**, *29*, 858–862.
- (34) McDonald, J. C.; Duffy, D. C.; Anderson, J. R.; Chiu, D. T.; Wu, H.; Schueller, O. J. A.; Whitesides, G. M. Fabrication of microfluidic systems in polydimethyl siloxane. *Electrophoresis* **2000**, *21*, 27–40.
- (35) Massey, S.; Duboin, A.; Mantovani, D.; Tabeling, P.; Tatoulian, M. Stable modification of PDMS surface properties by plasma polymerization: innovative process of allylamine PECVD deposition and microfluidic devices sealing. *Surf. Coat. Technol.* **2012**, *206*, 4303–4309.
- (36) Bartolo, D.; Degré, G.; Ngheb, P.; Studer, V. Microfluidic stickers. *Lab Chip* **2008**, *8*, 274–279.
- (37) Marasso, S.; Giuri, E.; Canavese, G.; Castagna, R.; Quaglio, M.; Ferrante, I.; Perrone, D.; Cocuzza, M. A multilevel lab on chip platform for DNA analysis. *Biomed. Microdev.* **2011**, *13*, 19–27.
- (38) Pitts, J. N., Jr.; Letsinger, R. L.; Taylor, R. P.; Patterson, J. M.; Recktenwald, G.; Martin, R. B. Photochemical reactions of benzophenone in alcohols. *J. Am. Chem. Soc.* **1959**, *81*, 1068–1077.